AFRL-AFOSR-VA-TR-2021-0106

The hybridized discontinuous Galerkin method for implicit Large Eddy Simulations of Magnetohydrodynamic Flows

Peraire, Jaime
MASSACHUSETTS INSTITUTE OF TECHNOLOGY
77 MASSACHUSETTS AVE
CAMBRIDGE, MA, 2139
USA

08/17/2021
Final Technical Report

DISTRIBUTION A: Distribution approved for public release.

Air Force Research Laboratory
Air Force Office of Scientific Research
Arlington, Virginia 22203
Air Force Materiel Command

REPORT DOCUMENTATION PAGE	*Form Approved* *OMB No. 0704-0188*

1. REPORT DATE *(DD-MM-YYYY)*	**2. REPORT TYPE**	**3. DATES COVERED** *(From - To)*
17-08-2021	Final	01 Jun 2016 - 31 May 2020

4. TITLE AND SUBTITLE The hybridized discontinuous Galerkin method for implicit Large Eddy Simulations of Magnetohydrodynamic Flows	**5a. CONTRACT NUMBER**
	5b. GRANT NUMBER FA9550-16-1-0214
	5c. PROGRAM ELEMENT NUMBER 61102F
6. AUTHOR(S) Jaime Peraire	**5d. PROJECT NUMBER**
	5e. TASK NUMBER
	5f. WORK UNIT NUMBER
7. PERFORMING ORGANIZATION NAME(S) AND ADDRESS(ES) MASSACHUSETTS INSTITUTE OF TECHNOLOGY 77 MASSACHUSETTS AVE CAMBRIDGE, MA 2139 USA	**8. PERFORMING ORGANIZATION REPORT NUMBER**
9. SPONSORING/MONITORING AGENCY NAME(S) AND ADDRESS(ES) AF Office of Scientific Research 875 N. Randolph St. Room 3112 Arlington, VA 22203	**10. SPONSOR/MONITOR'S ACRONYM(S)** AFRL/AFOSR RTA2
	11. SPONSOR/MONITOR'S REPORT NUMBER(S) AFRL-AFOSR-VA-TR-2021-0106

12. DISTRIBUTION/AVAILABILITY STATEMENT
A Distribution Unlimited: PB Public Release

13. SUPPLEMENTARY NOTES

14. ABSTRACT
We develop hybridized discontinuous Galerkin (HDG) methods for ideal and resistive compressible magnetohydrodynamics (MHD. The methods are fully implicit, high-order accurate and reduce the globally coupled unknowns to the approximate trace of the solution on element boundaries. Furthermore, we develop a shock capturing method to deal with shocks by appropriately adding artificial bulk viscosity, molecular viscosity, thermal conductivity, and electric resistivity to the physical viscosities in the MHD equations. In a step towards a full MHD Large-Eddy Simulation (LES) capability, we develop high-order Implicit LES approaches for transitional flows. Various turbulence phenomena are predicted and demonstrated, such as periodic low-frequency oscillations of shock wave in the streamwise direction, strong shear layer-detached from the shock wave due to shock wave boundary layer interaction and shock-induced flow separation. In order to exploit the hardware advances in GPU architectures we develop a matrix-free solution approach which has been implemented on GPU computers.

15. SUBJECT TERMS

16. SECURITY CLASSIFICATION OF:			**17. LIMITATION OF ABSTRACT**	**18. NUMBER OF PAGES**	**19a. NAME OF RESPONSIBLE PERSON** FARIBA FAHROO
a. REPORT	**b. ABSTRACT**	**c. THIS PAGE**			**19b. TELEPHONE NUMBER** *(Include area code)*
U	U	U	UU	12	426-8429

Standard Form 298 (Rev.8/98)
Prescribed by ANSI Std. Z39.18

REPORT DOCUMENTATION PAGE

Form Approved
OMB No. 0704-0188

1. REPORT DATE *(DD-MM-YYYY)*
10/08/2020

2. REPORT TYPE
Final

3. DATES COVERED *(From - To)*
6/1/16- 5/31/20

4. TITLE AND SUBTITLE
(YIP) The Hybrid Discontinuous Galerkin Method for Implicit Large Eddy Simulations of Manetohydrodynamic Flows

5a. CONTRACT NUMBER

5b. GRANT NUMBER
FA9550-16-1-0214

5c. PROGRAM ELEMENT NUMBER

6. AUTHOR(S)
Jaime Peraire and Ngoc. C. Nguyen

5d. PROJECT NUMBER

5e. TASK NUMBER

5f. WORK UNIT NUMBER

7. PERFORMING ORGANIZATION NAME(S) AND ADDRESS(ES)
Massachusetts Institute of Technology
77 Massachusetts Avenue
Cambridge, MA. 02129

8. PERFORMING ORGANIZATION REPORT NUMBER

9. SPONSORING / MONITORING AGENCY NAME(S) AND ADDRESS(ES)
Office of Naval Research
Boston Regional Office/N62879
495 Summer Street
Boston, MA 02210

10. SPONSOR/MONITOR'S ACRONYM(S)
ONR

11. SPONSOR/MONITOR'S REPORT NUMBER(S)

12. DISTRIBUTION / AVAILABILITY STATEMENT
unlimited

13. SUPPLEMENTARY NOTES

14. ABSTRACT
We develop hybridized discontinuous Galerkin (HDG) methods for ideal and resistive compressible magnetohydrodynamics (MHD. The methods are fully implicit, high-order accurate and reduce the globally coupled unknowns to the approximate trace of the solution on element boundaries. Furthermore, we develop a shock capturing method to deal with shocks by appropriately adding artificial bulk viscosity, molecular viscosity, thermal conductivity, and electric resistivity to the physical viscosities in the MHD equations. In a step towards a full MHD Large-Eddy Simulation (LES) capability, we develop high-order Implicit LES approaches for transitional flows. Various turbulence phenomena are predicted and demonstrated, such as periodic low-frequency oscillations of shock wave in the streamwise direction, strong shear layer-detached from the shock wave due to shock wave boundary layer interaction and shock-induced flow separation. In order to exploit the hardware advances in GPU architectures we develop a matrix-free solution approach which has been implemented on GPU computers.

15. SUBJECT TERMS
Discontinuous Galerkin Methods, Magnetohydrodynamics, Large Eddy Simulation, Flow Transition, GPU computing.

16. SECURITY CLASSIFICATION OF:			17. LIMITATION OF ABSTRACT	18. NUMBER OF PAGES	19a. NAME OF RESPONSIBLE PERSON
a. REPORT	b. ABSTRACT	c. THIS PAGE			19b. TELEPHONE NUMBER *(include area code)*

Standard Form 298 (Rev. 8-98)
Prescribed by ANSI Std. Z39.18

THE HYBRIDIZED DISCONTINUOUS GALERKIN METHOD FOR IMPLICIT LARGE EDDY SIMULATIONS OF MAGNETOHYDRODYNAMIC FLOWS

J. Peraire and C. N. Nguyen
Department of Aeronautics and Astronautics, Massachusetts Institute of Technology

FINAL REPORT
AFOSR Grant: FA9550-16-1-0214
Period covered: 6/1/16-5/31/20
Program Manager: Fariba Fahroo (Computational Mathematics)

Title: The hybridized discontinuous Galerkin method for implicit Large Eddy Simulations of Magnetohydrodynamic Flows

Discontinuous Galerkin (DG) methods have attracted considerable attention because they possess desirable properties for solving hyperbolic systems of conservation laws. The DG methods work well on arbitrary meshes, result in stable high-order discretization of the convective and diffusive operators, allow for a simple and unambiguous imposition of boundary conditions, and are well-suited to adaptive strategies. A class of DG methods that produce more accurate approximations and results in global systems with a reduced number of gloablly coupled degrees of freedom is the Hybdiridzed Discontinuous Galerkin (HDG) methods. HDG methods were first introduced in [1] and later extended in [2], [3], [4], [5], [6], [7], [8], [9]. The essential ingredients are a local Galerkin projection of the underlying PDEs at the element level onto spaces of polynomials of degree k to parametrize the numerical solution in terms of the numerical trace; a judicious choice of the numerical flux to provide stability and consistency; and a global jump condition that enforces the continuity of the numerical flux to arrive at a global weak formulation in terms of the numerical trace. The first HDG method for the compressible Euler and Navier-Stokes equations was introduced in [10]. This method possesses a number of desirable properties. First, in implicit formulations, it reduces the globally coupled unknowns to the numerical trace of the solution on element boundaries, thereby leading to a significant reduction in the degrees of freedom. Second, it provides, for smooth (e.g., viscous-dominated) problems, approximations for all the variables which converge with the optimal order of $k+1$ in the L^2-norm. And, third, it possesses superconvergence properties that allow us to compute a new approximate velocity which converges with order $k+2$ for $k \geq 1$.

One of the main outcomes of this grant has been the development of hybridized discontinuous Galerkin (HDG) methods for ideal and resistive compressible magnetohydrodynamics (MHD) [16]. The HDG methods for the MHD equations are fully implicit, high-order accurate and, as with other applications of HDG methods, they reduce the globally coupled unknowns to the approximate trace of the solution on element boundaries, thereby resulting in considerably smaller global degrees of freedom than other DG methods. Furthermore, we have developed a shock capturing method to deal with shocks by appropriately adding artificial bulk viscosity, molecular viscosity, thermal conductivity, and electric resistivity to the physical viscosities in the MHD equations [14], [16]. We have shown the optimal convergence of the HDG methods for ideal MHD problems and validate our resistive implementation for a magnetic reconnection problem. For smooth problems, we have observed that employing a generalized Lagrange multiplier (GLM) formulation can reduce the errors in the divergence of the magnetic field by two orders of magnitude. We have demonstrated the robustness of our shock capturing method on a number of test cases and compare our results, both qualitatively and quantitatively, with other MHD solvers. For shock problems, we have observed that an effective treatment of both the shock wave and the divergence-free constraint is crucial to ensuring numerical stability.

In many applications of interest, MHD flows experience transition from laminar to turbulence and pose unique computational challenges that must be addressed specifically. These include the interaction of fluids and electromagnetic fields, small-scale anisotropy, energy transfer among various scales between the velocity and magnetic field, and magnetic reconnection. In a step towards a full MHD-ILES capability, we have developed high-order Implicit Large-Eddy Simulation (ILES) approaches for transitional flows and applied them to perform wall-resolved implicit large eddy simulations [11], [12], [13]. The methods encompass an implicit Discontinuous Galerkin (DG) method for the discretization of the Navier–Stokes (NS) equations, and a parallel preconditioned Newton-GMRES solver for the resulting nonlinear system of equations [15]. In order to effectively resolve the boundary layers at high Reynolds numbers, we use a mesh refinement strategy to provide adequate resolution in the boundary layer region to capture flow transition and onset of turbulence. Various turbulence phenomena are predicted and demonstrated, such as periodic low-frequency oscillations of shock wave in the streamwise direction, strong shear layer-detached from the shock wave due to shock wave boundary layer interaction (SWBLI) and small scale structures broken down by the shear layer instability in the transition region, and shock-induced flow separation. In order to exploit the hardware advances in GPU architectures we have developed a matrix-free solution approach which has been implemented on GPU computers and enabled the large scale simulations performed during the period of this grant.

Below, we summarize the main research accomplishments. In particular, we describe the development and validation work of our MHD solver, the development of a matrix-free solver for conservation laws suitable for GPU implementation, and the application of our matrix-free solver to the solution of a wall-resolved transonic LES flow over an airfoil section [27], [28].

I. Research Results

A. *Implicit Hybridized Discontinuous Galerkin Methods for Compressible Magnetohydrodynamics*

We have developed implicit hybridized discontinuous Galerkin (HDG, EDG and IEDG) methods for ideal and resistive compressible magnetohydrodynamics (MHD) [16]. We have shown optimal convergence of the schemes for two smooth ideal MHD problems and validated our resistive implementation for a magnetic reconnection problem. For smooth problems, we show that using the Lagrange multiplier can reduce the errors in the divergence of the magnetic field by two orders of magnitude. For nonsmooth problems, we extend the shock capturing method presented previously developed to deal with shocks, contact discontinuities, and other unresolved features (such as strong current sheets, shear layers and thermal gradients). Our shock capturing method is based on the addition of physics-based artificial bulk viscosity, molecular viscosity, thermal conductivity, and electric resistivity to the MHD equations [14], [16]. The amount of artifical viscosity is determined by ensuring cell Péclet numbers of order unity. We demonstrate the robustness of our shock capturing method on a number of test cases and compare our results, both qualitatively and quantitatively, against other MHD solvers. For shock problems, we show that the divergence cleaning becomes an essential step in ensuring numerical stability.

The MHD equations are a system of nonlinear conservation laws for the mass, momentum, energy and magnetic field together with a divergence-free constraint on the magnetic field. In reality, the exact integration of the MHD conservation laws preserves the zero divergence of the magnetic field, if the initial condition is divergence-free. For this reason, the divergence-free condition is sometimes called an involution rather than a constraint. Unfortunately, when the MHD conservation laws are solved numerically, the divergence of the magnetic field obtained is typically not zero. It turns out that inadequate preservation of this property may lead to numerical instabilities and nonphysical features in the approximations. Many techniques have been proposed to enforce the divergence-free condition or reduce the divergence-error in the numerical solution. They include the eight-wave methods, the projection method, the hyperbolic divergence cleaning methods. In our work we have used a generalized Lagrange multiplier for hyperbolic divergence cleaning.

We have validated our method with several examples. The Orszag-Tang vortex is a second example that was initially proposed as a test case to study 2D MHD turbulence and was later adopted by the numerical analysis community as the go-to test case for MHD shock capturing due to its complex shock pattern. We use this problem since it allows us to test transition to supersonic MHD turbulence, the formation of shocks, shock-shock interactions, plasma tearing instabilities and the effect of divergence cleaning. For the solution of this problem, we use the HDG scheme with $k = 6$ and a grid of 128×128 quadrilaterals.

In Figure 1, we track visually the evolution of the solution. Shocks quickly develop from the smooth initial conditions and start interacting; actually the interaction of 3 shocks leads to the formation of a central current sheet. This current sheet undergoes a tearing instability which leads to the formation of plasmoids which move along the current sheet, coalesce and eventually die away.

In Figure 2, we compare our results against those obtained using Athena in and a 512×512 grid. Athena is an open source 3rd order reconstruction FV solver using HLLC Riemann fluxes used for astrophysical simulations. We also note that Athena uses constrained transport reconstruction for the magnetic field, and hence it enforces exactly the zero-divergence of the magnetic field. We can see that the results match extremely well suggesting that our shock capturing method removes all spurious oscillations and gives very sharp shock profiles.

B. GPU-Accelerated Implicit Discontinuous Galerkin Discretization

We have developed and implemented a matrix-free implicit DG solver on GPUs using CUDA and MPI. To solve the large linear systems of equations generated at each timestep, our DG solver is equipped with a matrix-free preconditioner using the reduced basis method and low rank updates to the approximate Jacobian [18], [19].

In order to assess the performance of our code, we conduct a few benchmarks and in-depth profiling runs on shared-memory systems. We have chosen a Nvidia Titan V GPU with a theoretical peak performance of 7.45 TFLOP/s and a maximum bandwidth of 652GB/s, and an Intel Xeon E5 2660 v3 CPU (10 cores) with a theoretical peak performance of 528 GFLOP/s and a maximum bandwith of 68GB/s. In Figure 3, we present scaled run times for the CPU and GPU for different values of the approximating polynomial degree p. The results show a very significant performance gain for the Titan V GPU, that varies between a factor of 16 for $p = 4$ and 12.5 for $p = 2$. Our algorithms result in increasing operation counts for higher polynomial orders, while on the other hand low polynomial orders are compromised by a less efficient memory access. Our GPU code is generally memory bandwidth bound, with a utilization rate of about 90%. For the lowest polynomial orders, the smaller array sizes lead to less ideal memory access patterns and hence lower bandwidth. For the CPU, the achieved bandwidth is around 45% of the theoretical maximum, indicating there is no clear performance bottleneck.

Figure 4 shows the weak and strong scaling of our DG code using up to 768 nodes at the OLCF's Summit supercomputer with access provided through a Director's Discretionary Allocation. The results correspond to a DNS simulation. The numerical discretization is based on third-order DG and DIRK timestepping schemes. One MPI rank per GPU was used. For the strong scaling assessment, a fully resolved grid of approximately 12 million fourth-order elements was partitioned in 144, 288, 576, 1152, 2304, 4608 subdomains.

From Figure 4, excellent weak scaling is observed up to 768 nodes. In particular, performance degrades by about 5% when scaling from 24 to 768 nodes. Similar observations can be made for the strong scaling

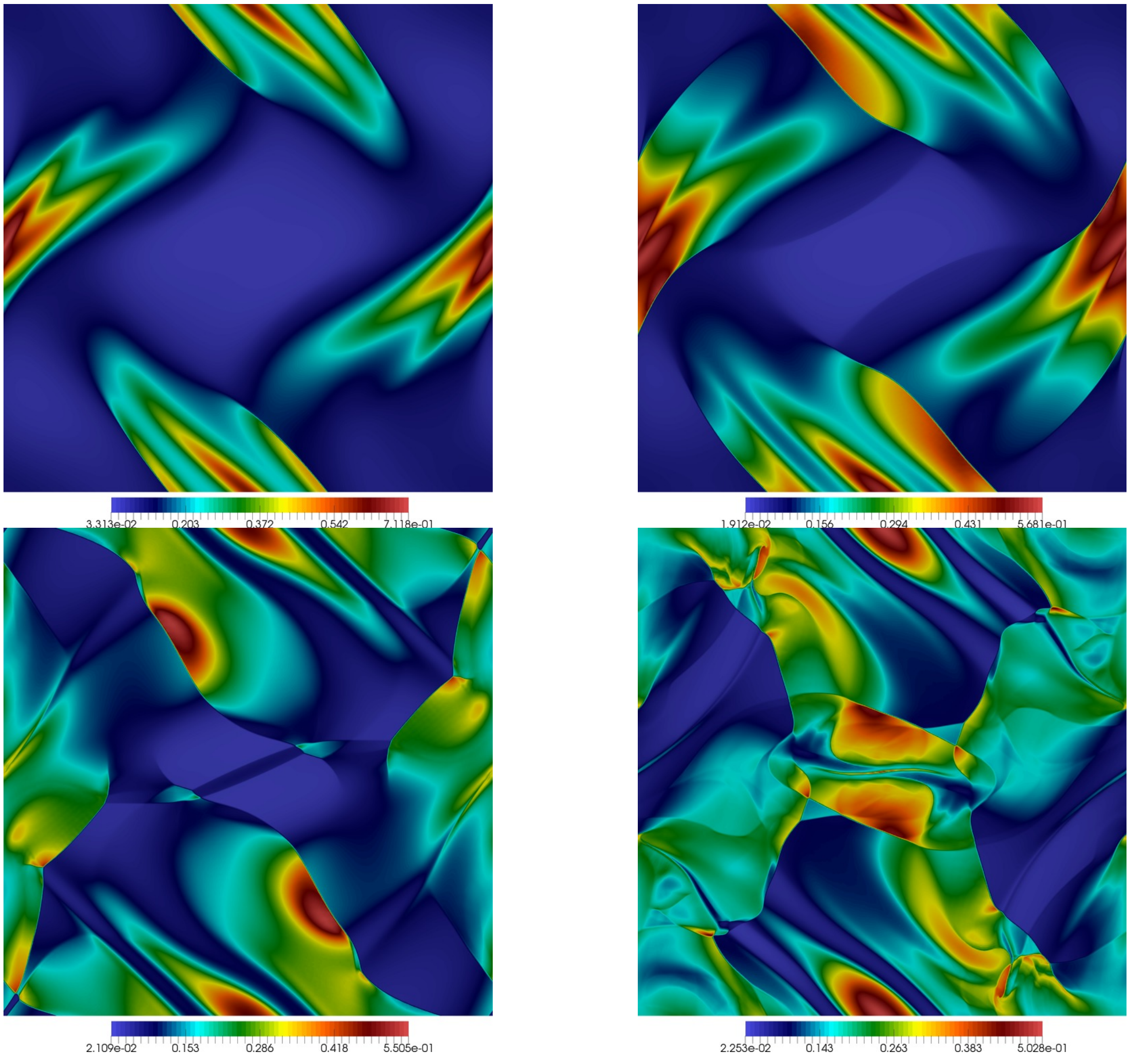

Fig. 1. Evolution of the Orszag-Tang Vortex problem. We show pressure at times (from top to bottom, left to right) $t = 0.176$, $t = 0.234$, $t = 0.352$, $t = 0.508$.

test. Specifically, we obtain excellent strong scaling up to 768 nodes and the scaling performance degrades very slowly as the number of nodes increases. The scaling results show that our code has the potential to maintain good scaling performance up to several thousand nodes.

C. Wall-Resolved Large Eddy Simulation

To demonstrate the capabilities of our GPU-based, matrix-free solver, we consider the transonic separated flow over an airfoil section at a Reynolds number of 3 million. In the classical (explicit) LES approach, the large-scale eddies of the flow field are resolved and the small scales are modeled using an appropriate SGS model. It turns out that the truncation error introduced by some numerical schemes is similar in form and magnitude to conventional SGS models and, in fact, some numerical schemes achieve stability by introducing stabilization terms, or truncation errors, that replicate the effect of the subgrid scales on the resolved scales [20]. A natural alternative to the SGS-based LES approach is to use the numerical

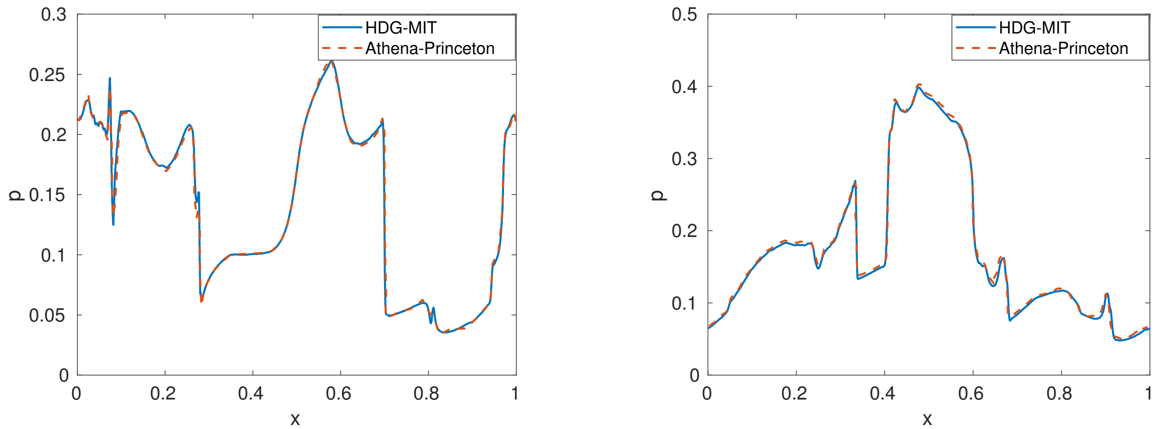

Fig. 2. Comparison between the HDG scheme presented here and the Athena solver for the Orszag-Tang vortex at $t = 0.5$. We show slices of dimensionless pressure at $y = 0.3125$ (left) and $y = 0.4277$ (right).

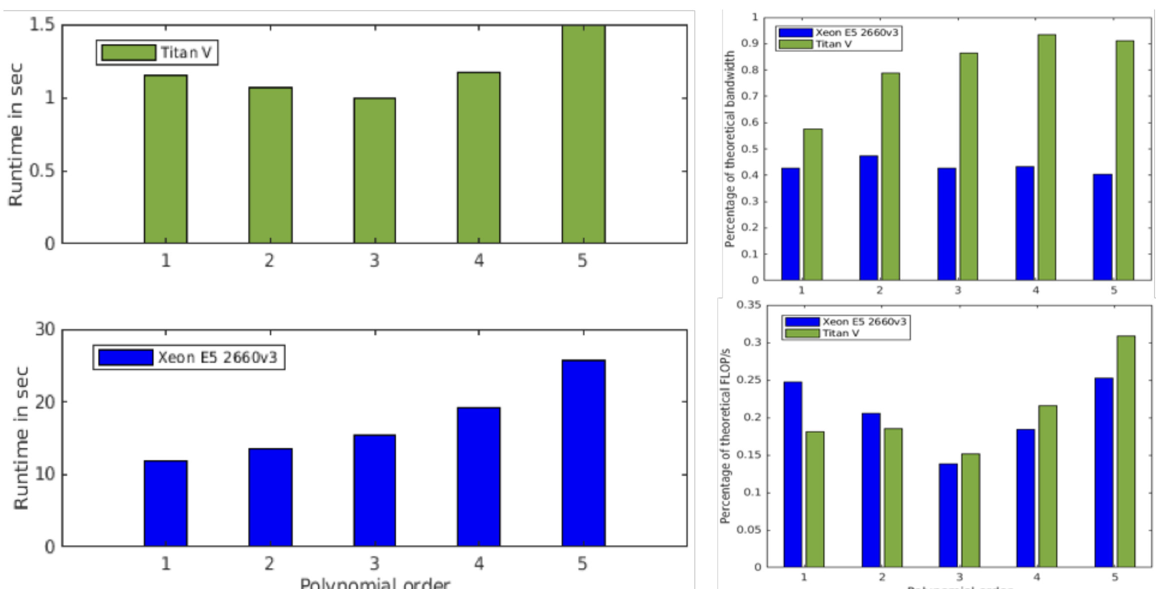

Fig. 3. *Runtime comparison between CPU and GPU for different polynomial degrees.*

dissipation of the discretization scheme to account for the dissipation that takes place in the unresolved scales, leading to implicit LES (ILES). ILES benefits from its easy implementation without a SGS model and currently gains considerable attention from researchers in the computational fluid dynamics (CFD) community [12]. As pointed out by Spalart [21], this increase in popularity may be attributed to the fact that research has failed to show an advantage of sophisticated SGS models over the same-cost LES with a simplistic model or even with no model and a slightly finer grid. We have investigated the ability of DG methods to accurately simulate under-resolved turbulent flows, and how to best account for the effect of the subgrid scales on the resolved scales from a practical and theoretical perspective. We have also analyzed the role of the Riemann solver and the subgrid scale model to predict a variety of flow regimes, including transition to turbulence, wall-free turbulence and wall-bounded turbulence. Numerical

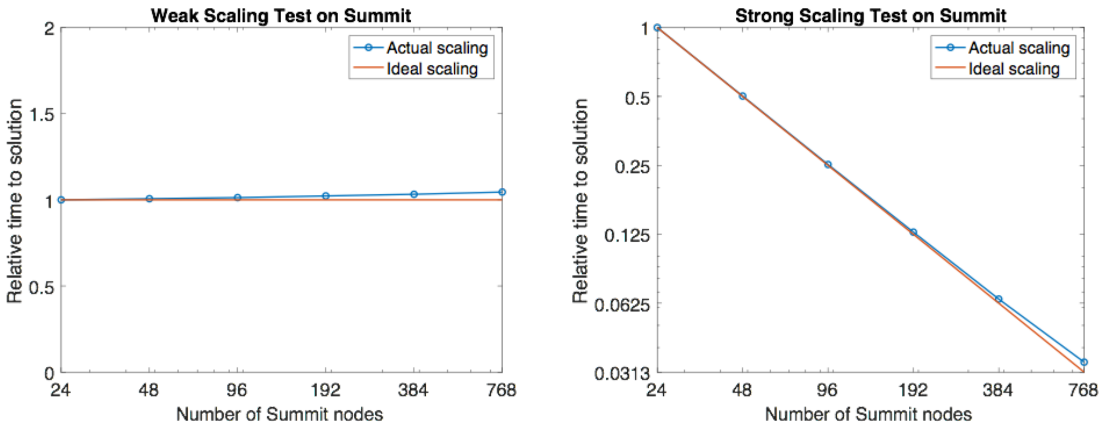

Nodes	DOFs	Time (s)	Time ratio
24	0.408 B	3.10	1.0000
48	0.816 B	3.12	1.0065
96	1.632 B	3.14	1.0129
192	3.264 B	3.17	1.0226
384	6.528 B	3.20	1.0323
768	13.056 B	3.25	1.0484

Nodes	DOFs	Time (s)	Time ratio
24	1.632 B	12.45	1.0000
48	1.632 B	6.25	0.502
96	1.632 B	3.14	0.252
192	1.632 B	1.59	0.128
384	1.632 B	0.811	0.065
768	1.632 B	0.43	0.035

Fig. 4. *Weak scaling (left) and strong scaling (right) tests of* `CAMPS` *on NVIDIA Tesla V100 GPUs at the OLCF's Summit supercomputer.*

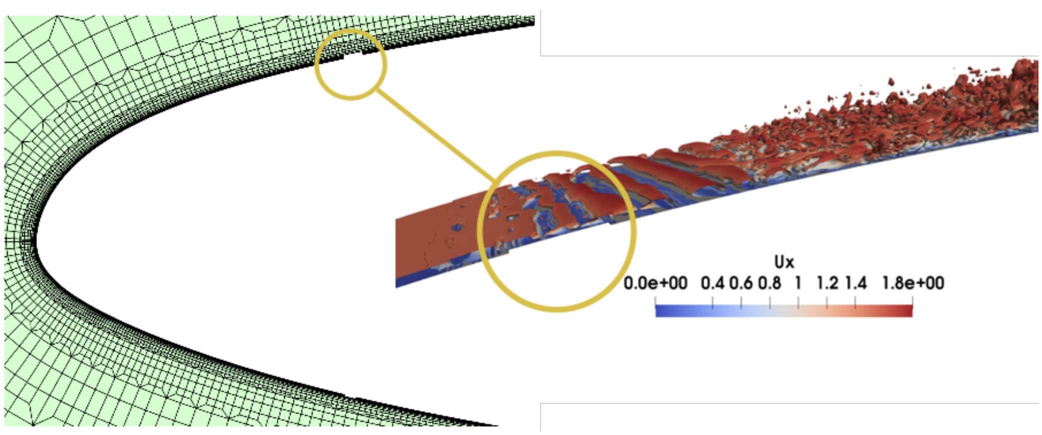

Fig. 5. Zoom of the mesh near the transition trips and the flow structure near the upper transition trip. It can be seen that the transition from laminar to turbulence occurs at the trip location. The numerical transition trips were modeled by using the dimensions of the real trips used in the experiment [23].

results show that DG methods have a built-in (implicit) subgrid scale model and introduce numerical dissipation in under-resolved turbulence simulations; thus, confirming the ab–initio separation of scales predicted by nonmodal analysis [22], [17]. For the test problems considered, the implicit model provides a more accurate representation of the subgrid scales in the flow than state–of–the–art explicit eddy viscosity

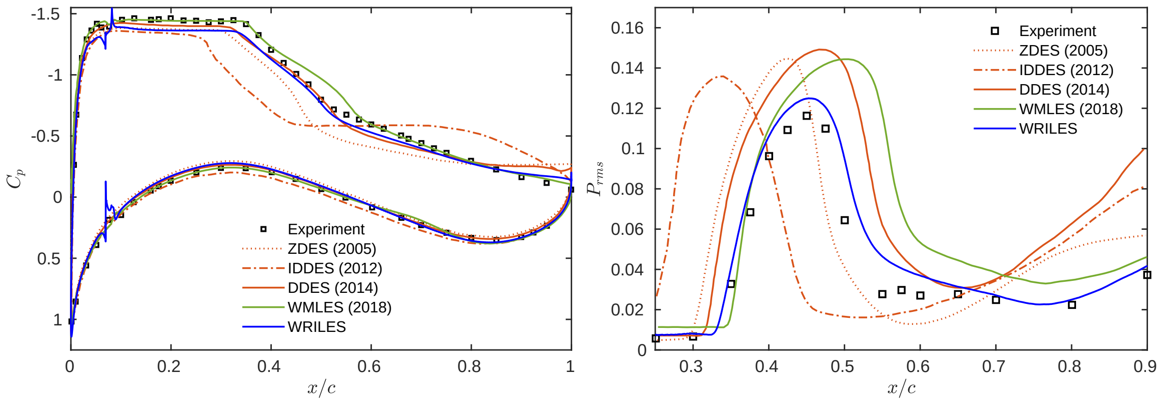

Fig. 6. Comparisons of the spanwise-and-time-averaged pressure coefficient on the airfoil surface (left) and wall pressure fluctuations on the suction surface (right). The WRILES predictions agree well with the experimental data [23]. The overshoots of the pressure coefficient around $x/c = 0.07$ obtained by the WRILES are due to the transition strips.

models, including dynamic Smagorinsky, WALE and Vreman. Implicit modeling also outperforms explicit modeling for laminar flows that do not contain subgrid scales; which is a critical feature to accurately predict transition to turbulence. Our analysis [22], [17] reveals that polynomial orders $p = 2, 3$ and 4 with standard upwinding are the most adequate for LES, at least in the implicit LES context. For lower polynomial orders, dissipation is introduced at scales that are larger than the grid resolution. We have also found that strong under/over–upwinding, as well as higher polynomial orders, may lead to numerical stability issues. Finally, we have observed that Riemann solvers that are based on the maximum–magnitude eigenvalue of the Jacobian matrix of the Euler fluxes, such as, the Lax–Friedrichs solver and the HLL solver, produce excessive over–upwinding in low Mach numbers regions.

We adopt a wall–resolved LES approach. The main advantage the wall-resolved LES approach is the accurate representation of the flow transition mechanisms. It turns out that the overall flow field is extremely sensitive to the transition location, while the fine details of the turbulent flow have a much lesser impact on the time averaged quantities which are typically of interest. This point is illustrated with the simulation of the flow over a supercritical OAT15A wing at $Re = 3 \times 10^6$, $M_\infty = 0.73$, and 3.5^o angle of attack (AoA), which was experimentally studied in [23]. This flow exhibits strong buffeting with low frequency limit cycle oscillations. The simulation demands over a million timesteps (for 100 chord flow throughs). Our simulation is the first wall-resolved implicit LES of this turbulent flow, whereas previous work have considered turbulence models [24], [25] and wall-modeled LES [27]. Our simulation agrees well with experimental data [23], and indeed has better agreement with the experiment data than the wall–modeled LES computation [27], which had in excess of 440 million grid points (vs. 4.8 million grid points required by our simulation.) The mesh used for this study is made of 1.12 million quadratic hexahedra elements, which are potentially third order accurate. For a Discontinuous Galerkin method, it represents a total of approximately 30 million nodes. The 3D mesh is obtained by extruding a 2D mesh over $0.065c$ in the z-direction, by using 32 elements, i.e 96 nodes. The mesh geometry models the transition trips as steps (see Fig. 5), with dimensions equal to the experimental trips.

Comparisons with experimental data [23], as well as numerical other numerical simulations (ZDES [24], DDES [25], IDDES [26], and WMLES [27]) are shown in Fig. 6. The pressure coefficient and fluctuations obtained by the WRILES agree very well with the experimental data.

Figure 7 shows instantaneous streamwise velocity u_1 and instantaneous magnitude of the density gradient $||\nabla\rho||$ at different stages of the buffet cycle for the WRILES simulation. We observe the lambda structure of the shock foot in the instantaneous magnitude of the density gradient. Furthermore, we see

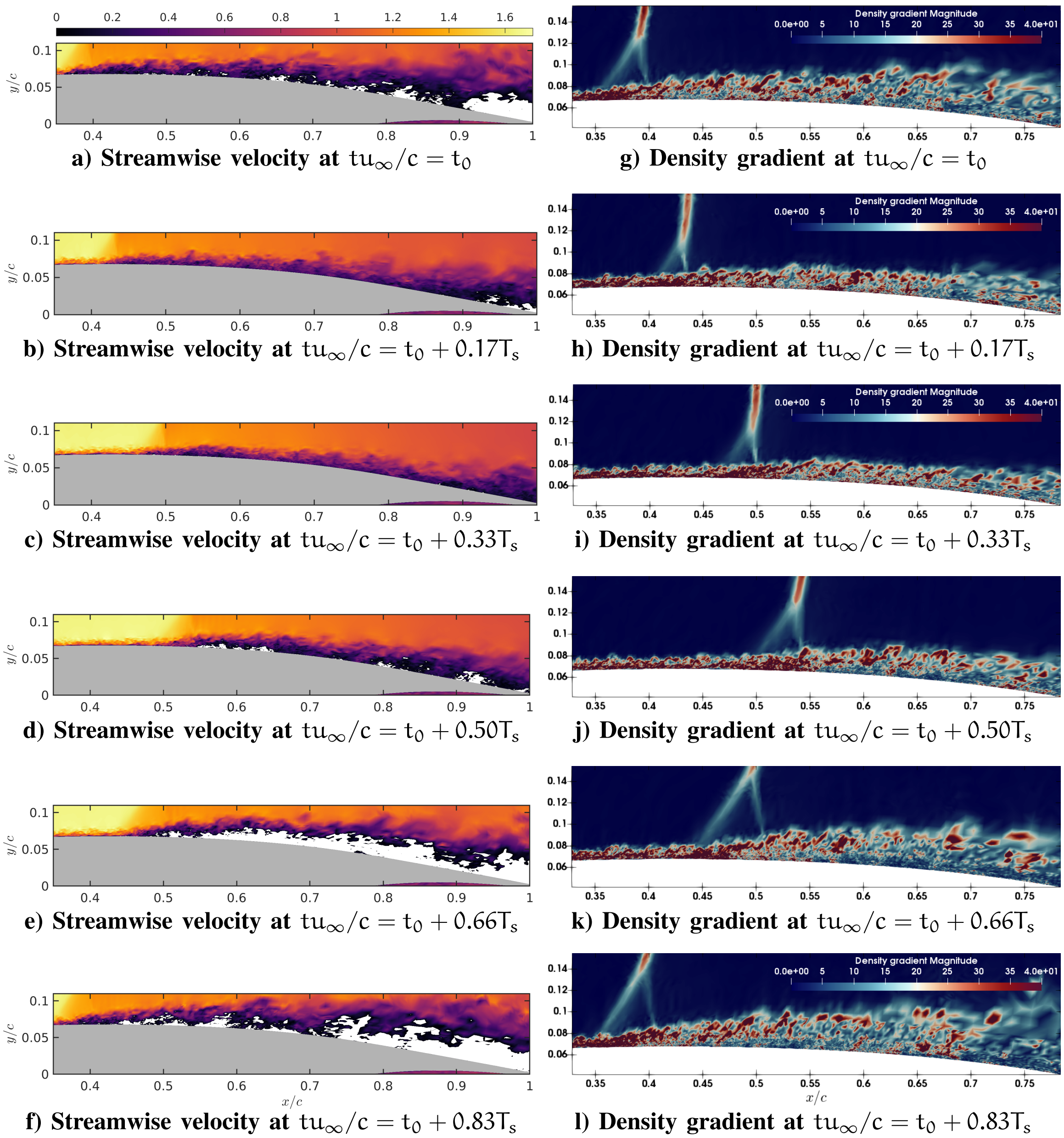

a) Streamwise velocity at $tu_\infty/c = t_0$
g) Density gradient at $tu_\infty/c = t_0$
b) Streamwise velocity at $tu_\infty/c = t_0 + 0.17T_s$
h) Density gradient at $tu_\infty/c = t_0 + 0.17T_s$
c) Streamwise velocity at $tu_\infty/c = t_0 + 0.33T_s$
i) Density gradient at $tu_\infty/c = t_0 + 0.33T_s$
d) Streamwise velocity at $tu_\infty/c = t_0 + 0.50T_s$
j) Density gradient at $tu_\infty/c = t_0 + 0.50T_s$
e) Streamwise velocity at $tu_\infty/c = t_0 + 0.66T_s$
k) Density gradient at $tu_\infty/c = t_0 + 0.66T_s$
f) Streamwise velocity at $tu_\infty/c = t_0 + 0.83T_s$
l) Density gradient at $tu_\infty/c = t_0 + 0.83T_s$

Fig. 7. Left column: instantaneous streamwise velocity u_1 at different stages of the buffet cycle. Right column: instantaneous magnitude of the density gradient $||\nabla\rho||$ at the same stages.

that the flow is strongly separated when the shock moves upstream and weakly separated when the shock moves down stream.

In order to visualize the vortex structures of the flow, Fig. 8 displays the isosurfaces of Q, the second invariant of the velocity gradient tensor. On Fig. 8, the isosurfaces are colored by the streamwise velocity, and a spanwise cross section of the Mach number field is also displayed in the background. At $x/c = 0.07$,

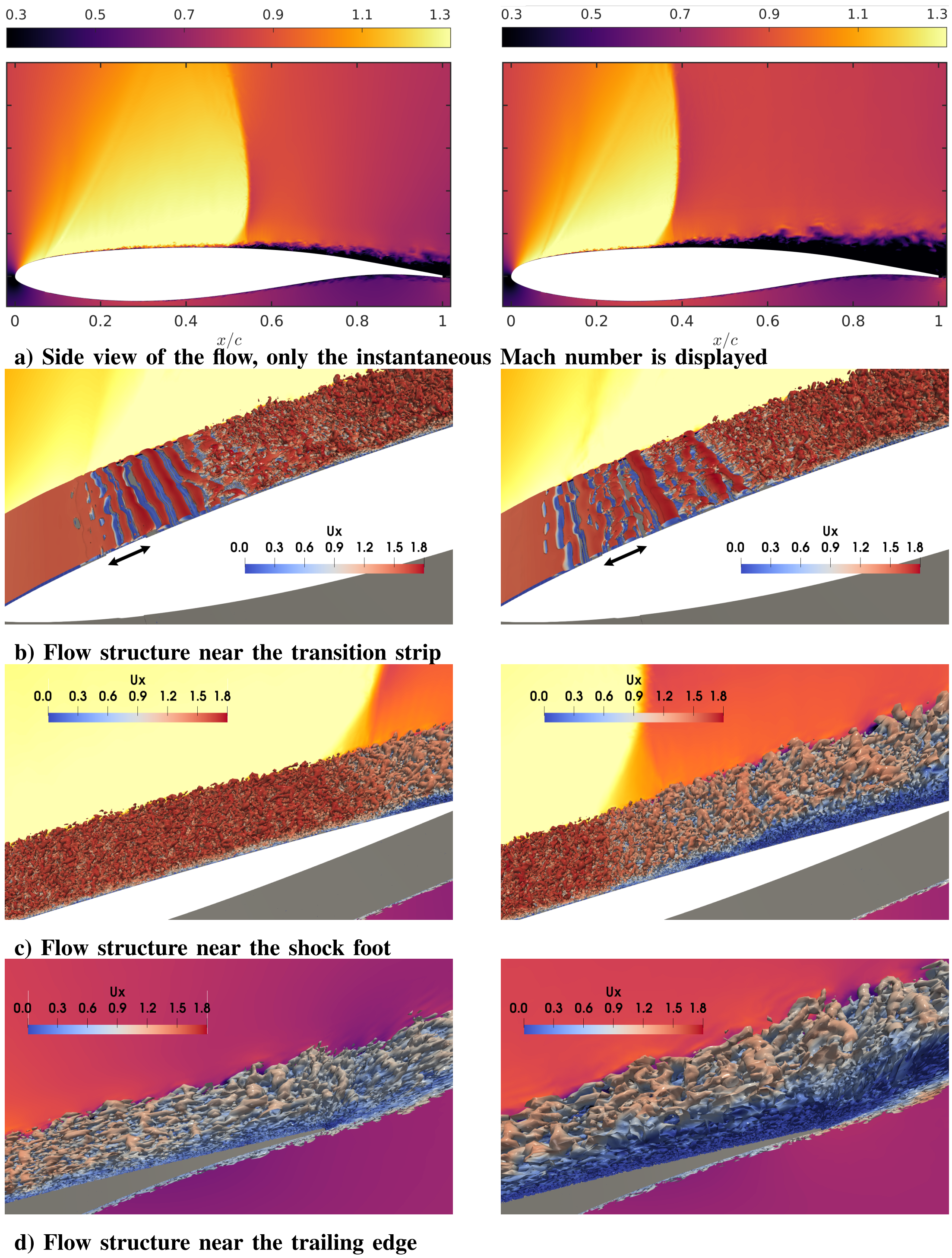

Fig. 8. Instantaneous Mach number at $z = 0$ and isosurfaces of Q-criterion ($Q/M_\infty^2 = 200$) colored by the streamwise velocity obtained by WRILES. Left column : maximal downstream shock location ($tu_\infty/c = t_0$). Right column: maximal upstream shock location ($t = t_0 + 0.5T_s$). On b), the strip width is indicated with an arrow.

the transition trip generates an expansion wave, visible on the Mach number plots (Fig. 8,a-b). Two-dimensional spanwise-coherent vortices are induced by the trip and immediately break down to smaller three-dimensional structures (Fig. 8,b). Quasi-streamwise vortices and irregular lambda-shape vortices are visible in the lower part of the boundary layer, where the two-dimensional vortices breaks down at $x/c \approx 0.10$. The transition happens very fast and the boundary layer seems fully turbulent for $x/c > 0.12$. Packets of hairpin-like vortices are visible in the shock foot area, and they grow toward the downstream (Fig. 8,c). As expected, the turbulent boundary layer significantly thickens after passing through the foot shock. From Fig. 8,d), it is clear that during the upstream excursion of the shock, the shear layer is thicker and completely separated downstream of the lambda shock, while during the downstream shock excursion, the shear layer is thinner and remains largely attached to the wall, except very locally at the trailing edge.

REFERENCES

[1] B. COCKBURN, J. GOPALAKRISHNAN, AND R. LAZAROV. Unified hybridization of discontinuous Galerkin, mixed and continuous Galerkin methods for second order elliptic problems. *SIAM J. Numer. Anal.*, 47, 1319–1365, 2009.

[2] N.-C. NGUYEN, J. PERAIRE, AND B. COCKBURN, *An implicit high-order hybridizable discontinuous Galerkin method for linear convection-diffusion equations*, J. Comput. Phys., 228 (2009), pp. 3232–3254.

[3] N.-C. NGUYEN, J. PERAIRE, AND B. COCKBURN, *An implicit high-order hybridizable discontinuous Galerkin method for nonlinear convection-diffusion equations*, J. Comput. Phys., 228 (2009), pp. 8841–8855.

[4] N.-C. NGUYEN, J. PERAIRE, AND B. COCKBURN, *A comparison of HDG methods for Stokes flow*, J. Sci. Comput., 45 (2010), pp. 215–237.

[5] N.-C. NGUYEN, J. PERAIRE, AND B. COCKBURN, *A hybridizable discontinuous Galerkin method for Stokes flow*, Comput. Methods Appl. Mech. Engrg., 199 (2010), pp. 582–597.

[6] N.-C. NGUYEN, J. PERAIRE, AND B. COCKBURN, *High-order implicit hybridizable discontinuous Galerkin methods for acoustics and elastodynamics*, J. Comput. Phys., 230 (2011), pp. 3695–3718.

[7] N.-C. NGUYEN, J. PERAIRE, AND B. COCKBURN, *Hybridizable discontinuous Galerkin methods for the time-harmonic Maxwell's equations*, J. Comput. Phys., 230 (2011), pp. 7151–7175.

[8] N.-C. NGUYEN, J. PERAIRE, AND B. COCKBURN, *An implicit high-order hybridizable discontinuous Galerkin method for the incompressible Navier-Stokes equations*, J. Comput. Phys., 230 (2011), pp. 1147–1170.

[9] J. PERAIRE, N. C. NGUYEN, AND B. COCKBURN., An Embedded Discontinuous Galerkin Method for the compressible Euler and Navier-Stokes equations (AIAA Paper 2011-3228). In *Proceedings of the 20th AIAA Computational Fluid Dynamics Conference*, Honolulu, Hawaii, June 2011.

[10] J. PERAIRE, N. C. NGUYEN, AND B. COCKBURN, *A hybridizable discontinuous Galerkin method for the compressible Euler and Navier-Stokes equations* (AIAA Paper 2010-363). In *Proceedings of the 48th AIAA Aerospace Sciences Meeting and Exhibit*, Orlando, Florida, January 2010.

[11] B. COCKBURN, N. C. NGUYEN, J. PERAIRE, *HDG Methods for Hyperbolic Problems*, Handbook of Numerical Analysis 17. (2016): 73 –197.

[12] P. FERNANDEZ, N. C. NGUYEN, J. PERAIRE, *The hybridized Discontinuous Galerkin method for Implicit Large-Eddy Simulation of transitional turbulent flows*, Journal of Computational Physics 336. (2017): 308-329.

[13] P. FERNANDEZ, N.C. NGUYEN, J. PERAIRE, *Sugbrid-scale modeling and implicit numerical dissipation in DG-based Large-Eddy Simulation*, 23rd AIAA Computational Fluid Dynamics Conference, AIAA 2017–3951, Denver, CO, Jun 2017.

[14] P. FERNANDEZ, N.C. NGUYEN, J. PERAIRE, *A physics-based shock capturing method for unsteady turbulent flows*, 56th AIAA Aerospace Sciences Meeting (SciTech 2018), Gaylord Palms, FL, Jan 2018. To appear.

[15] P.-O. PERSSON, J. PERAIRE, *Newton-GMRES Preconditioning for Discontinuous Galerkin Discretizations of the Navier–Stokes Equations*, SIAM Journal on Scientific Computing, 6, 2008.

[16] C. CIUCA, P. FERNANDEZ, A. CHRISTOPHE, N. C. NGUYEN, J. PERAIRE, *Implicit Hybridized Discontinuous Galerkin Methods for Compressible Magnetohydrodynamics*, J. Comp. Phys. X, vol. 5, 2020

[17] P. FERNANDEZ, N. C. NGUYEN, J. PERAIRE, *On the ability of discontinuous Galerkin methods to simulate under-resolved turbulent flows*, arXiv:1810.09435, 2018.

[18] N.C. NGUYEN, J. PERAIRE, *An efficient reduced-order modeling approach for non-linear parametrized partial differential equations*, International Journal for Numerical Methods in Engineering, 76, 2008.

[19] N. C. NGUYEN, P. FERNANDEZ, R. M. FREUND, AND J. PERAIRE *Accelerated residual methods for the iterative solution of systems of equations*, SIAM Journal on Scientific Computing, 40(5), 2018.

[20] T. J. R. HUGHES, L. MAZZEI, AND K. JANSEN, *Large Eddy Simulation and the variational multiscale method.* Comput. Visual. Sci., 3:47-59, 2000.

[21] P. R. SPALART, *Strategies for turbulence modelling and simulations. In International Journal of Heat and Fluid Flow*, volume 21, pages 252-263, 2000.

[22] P. FERNANDEZ, R. C. MOURA, G. MENGALDO, AND J. PERAIRE, *Non-modal analysis of spectral element methods: Towards accurate and robust large-eddy simulations*, Computer Methods in Applied Mechanics and Engineering, 346:43-62, 2019.

[23] L. JACQUIN, P. MOLTON, S. DECK, B. MAURY, AND D. SOULEVANT, *Experimental study of shock oscillation over a transonic supercritical profile*, AIAA Journal, 47(9):1985-1994, 2009.

[24] S. Deck, *Numerical simulation of transonic buffet over a supercritical Airfoil*, AIAA Journal, 43(7):1556-1566, 2005.
[25] F. Grossi, M. Braza, and Y. Hoarau, *Prediction of transonic buffet by delayed detached-eddy simulation*, AIAA Journal, 52(10):2300-2312, 2014.
[26] J. Huang, Z. Xiao, J. Liu, and S. Fu, *Numerical investigation of shock buffet on an OAT15A airfoil and control effects of vortex generators*, 50th AIAA Aerospace Sciences Meeting, 2012, pp. AIAA–2012–0044.
[27] Y. Fukushima and S. Kawai, *Wall-modeled large-eddy simulation of transonic airfoil buffet at high Reynolds number*, AIAA Journal, 56(6):2372-2388, 2018.
[28] N.C. Nguyen, S. Terrana and J. Peraire, *Wall-resolved implicit large eddy simulation of transonic buffet over the OAT15A airfoil using a discontinuous Galerkin method*, AIAA Scitech 2020 Forum, 2062.